

Targeted deletion of the ATP binding domain of left-right dynein confirms its role in specifying development of left-right asymmetries

Dorothy M. Supp^{1,‡,*}, Martina Brueckner^{2,*}, Michael R. Kuehn³, David P. Witte⁴, Linda A. Lowe³, James McGrath², JoMichelle Corrales² and S. Steven Potter^{1,¶}

¹Divisions of Molecular and Developmental Biology, The Children's Hospital Research Foundation, Cincinnati, Ohio, 45229, USA

²Department of Pediatrics/Cardiology, Yale School of Medicine, New Haven, Connecticut, 06520, USA

³Experimental Immunology Branch, National Cancer Institute, National Institutes of Health, Bethesda, Maryland, 20892, USA

⁴Department of Pathology, The Children's Hospital Medical Center, Cincinnati, Ohio, 45229, USA

*Joint first authorship

‡Current address: Research Department, Shriners Hospital for Children, Cincinnati, Ohio, 45229, USA

¶Author for correspondence (e-mail: steve.potter@chmcc.org)

Accepted 8 September; published on WWW 9 November 1999

SUMMARY

Vertebrates develop distinct asymmetries along the left-right axis, which are consistently aligned with the anteroposterior and dorsoventral axes. The mechanisms that direct this handed development of left-right asymmetries have been elusive, but recent studies of mutations that affect left-right development have shed light on the molecules involved. One molecule implicated in left-right specification is left-right dynein (LRD), a microtubule-based motor protein. In the LRD protein of the *inversus viscerum* (*iv*) mouse, there is a single amino acid difference at a conserved position, and the *lrd* gene is one of many genes deleted in the *legless* (*lgl*) mutation. Both *iv* and *lgl* mice display randomized left-right development. Here we extend the analysis of the *lrd* gene at the levels of sequence, expression and function. The complete coding sequence of the *lrd* gene confirms its classification as an axonemal, or ciliary, dynein. Expression of *lrd* in the node at embryonic day 7.5 is shown to be symmetric. At embryonic day 8.0, however, a striking asymmetric expression pattern is observed in all three germ layers of the developing headfold, suggesting roles in both the establishment and maintenance of left-right asymmetries.

At later times, expression of *lrd* is also observed in the developing floorplate, gut and limbs. These results suggest function for LRD protein in both ciliated and non-ciliated cells, despite its sequence classification as axonemal. In addition, a targeted mutation of *lrd* was generated that deletes the part of the protein required for ATP binding, and hence motor function. The resulting left-right phenotype, randomization of laterality, is identical to that of *iv* and *lgl* mutants. Gross defects in ciliary structure were not observed in *lrd/lrd* mutants. Strikingly, however, the monocilia on mutant embryonic node cells were immotile. These results prove the identity of the *iv* and *lrd* genes. Further, they argue that LRD motor function, and resulting nodal monocilia movement, are required for normal left-right development.

Movies available on-line:

<http://www.biologists.com/Development/movies/dev3019.html>

<http://genome.chmcc.org/cilia/>

Key words: Left-right asymmetry, Situs inversus, Dynein, ATP, Mouse

INTRODUCTION

Externally, vertebrates appear bilaterally symmetrical. However, internally they display characteristic and highly conserved asymmetries along the left-right (LR) axis. These include the positioning of the heart, stomach, pancreas and liver. In wild-type animals, LR asymmetries are consistently aligned relative to the anteroposterior (AP) and dorsoventral (DV) axes, but the molecular events that link existing AP and DV positional information to establish invariant LR visceral handedness are not yet well understood.

Determination of the vertebrate LR embryonic axis occurs well before the first morphological sign of LR asymmetry, the

rightward looping of the embryonic heart tube. The first signs of LR asymmetry are at the molecular level. Several genes with LR asymmetric expression patterns have been identified including *sonic hedgehog* (*Shh*), *HNF 3 β* , *activin receptor IIA* (*cActRIIA*), *cNRI* (*nodal-related 1*), *activin β B*, *Pitx2* and *cSnR* in the chick (Levin et al., 1995, 1997; Yoshioka et al., 1998; Logan et al., 1998; Piedra et al., 1998; Isaac et al., 1997), *nodal*, *lefty-1*, *lefty-2*, *Pitx2* and *SnR* in the mouse (Collignon et al., 1996; Lowe et al., 1996; Meno et al., 1996, 1998; Piedra et al., 1998; Yoshioka et al., 1998; Campione et al., 1999; Sefton et al., 1998), and *Xnr-1* and *Pitx2* in *Xenopus* (Lowe et al., 1996; Ryan et al., 1998). Although these have suggested a cascade of lateralized signaling eventually specifying LR

morphological asymmetries, where and when the initial breaking of symmetry occurs is unknown. The embryonic node, known as Hensen's node in chick and the Spemann organizer in *Xenopus*, has been shown to be essential to the development of LR asymmetry (Pagan-Westphal and Tabin, 1998; Hyatt and Yost, 1998) and is where the earliest asymmetric gene expression is seen. However, results from chick and *Xenopus* studies have suggested that positional information is initially provided to the node by adjacent tissue. Subsequently, the node signals LR instructions to more distant tissues, including the lateral plate mesoderm (Pagan-Westphal and Tabin, 1998; Hyatt and Yost, 1998). Experimental or genetic ablation of the notochord and floor plate of the neural tube indicate that these midline structures also play a key role in LR development (Danos and Yost, 1995, 1996; Lohr et al., 1997; Goldstein et al., 1998).

In the mouse, insight into laterality determination has come from analysis of the *situs inversus viscerum* (*iv*) mouse mutation (Hummel and Chapman, 1959). Adult *iv/iv* mutants have a roughly 50% incidence of inverted visceral organ positioning, suggesting that the gene product drives normal laterality and, in its absence, the process is randomized (Layton, 1976). The *iv* mutation disrupts the expression patterns of the asymmetric genes *nodal* (Lowe et al., 1996), *lefty* (Meno et al., 1996) and *Pitx2* (Piedra et al., 1998; Campione et al., 1999) indicating that the *iv* gene plays a critical early role in the genetic hierarchy of LR development. The *legless* (*lgl*) transgene insertional mutation is allelic to the *iv* mutation, but has a much more severe phenotype, including hindlimb truncations and craniofacial defects (McNeish et al., 1990). Molecular analysis indicated that the *lgl* mutation resulted in the deletion of over 600 kb of mouse genomic DNA (Supp et al., 1996, 1997). The different phenotypes seen in *iv* and *lgl* may result from different types of mutations or the deletion of multiple genes in *lgl*.

A good candidate for the *iv* gene was cloned from the *lgl* deletion region, a dynein heavy chain gene which we named *left-right dynein* (*lrd*). Dyneins are microtubule-based motors that use the energy of ATP hydrolysis to generate minus-end directed motive force in the sliding of adjacent microtubules in ciliary axonemes and the transport of multiple cargoes within the cytoplasm (reviewed by Holzbaur and Vallee, 1994). A human syndrome affecting LR development further implicated dyneins in specification of the LR asymmetries. Kartagener syndrome is characterized by a roughly 50% incidence of situs inversus (complete reversal of the LR axis), as well as dynein defects in the cilia that result in chronic respiratory infections and immotile sperm (Afzelius, 1976; Splitt et al., 1996). Further suggestion that molecular motors, and perhaps cilia, are involved in LR specification comes from the targeting of the mouse genes *kif3A* and *kif3B*. Mutations of *kif3A* or *kif3B*, members of the kinesin superfamily of motor proteins, result in absence of monocilia on cells of the embryonic node and defects in LR asymmetry (Marszalek et al., 1999; Takeda et al., 1999; Nonaka et al., 1998). Interestingly, expression of *lrd* was noted in the embryonic node (Supp et al., 1997).

In this report, we extend our analysis of the role of *lrd* in LR development. The complete *lrd* cDNA has been cloned and sequenced, confirming the classification of *lrd* as an axonemal dynein heavy chain gene. This is the first report of the full coding sequence of an axonemal dynein heavy chain gene in

vertebrates. A more extensive analysis of expression reveals that, in addition to symmetric expression in the embryonic node, apparently transient asymmetric expression of *lrd* occurs in the headfold region of 0- to 5-somite wild-type mouse embryos. At later stages, *lrd* is expressed symmetrically in the floorplate of the neural tube, a midline signaling center and a region of the embryo shown to be involved in LR development at earlier stages. To confirm the role of *lrd* in laterality, to test for possible involvement in other developmental processes and to begin to define the molecular mechanism of *lrd* function, a targeted mutation in the *lrd* gene was generated and the resulting mice characterized.

MATERIALS AND METHODS

Cloning *lrd* cDNA

Direct cDNA selection (Supp et al., 1997), reverse transcription polymerase chain reaction (RT-PCR) and rapid amplification of cDNA ends (RACE) (Marathon cDNA Amplification Kit, Clontech) were used to clone *lrd* cDNA sequences from wild-type adult mouse brain RNA. The cloned cDNA is 14,072 base pairs (bp) long, including 13,464 bp of coding sequence, 211 bp of 5' untranslated region (UTR), and 397 bp of 3' UTR. The putative translational start site is preceded by stop codons in all three reading frames. The coding sequence has been submitted to GenBank (accession number AF183144). For analysis of *lrd* cDNA in *iv/iv* mice, cDNAs were isolated from *iv/iv* mouse brain RNA using RT-PCR.

In situ hybridization

Serial section in situ hybridizations were performed as described (Supp et al., 1997) with an *lrd* antisense riboprobe spanning nucleotides 9,631-10,325 of the *lrd* cDNA sequence. Whole-mount in situ hybridizations were performed as described (Lowe et al., 1996) using an *lrd* antisense riboprobe spanning nucleotides 306-1,216 of the *lrd* cDNA sequence. Control hybridizations with sense-strand riboprobes showed no signal.

Gene targeting

The backbone targeting vector, *pMJK-KO*, was provided by Dr Michael Kern (S. C. Medical College). This vector contains the *pMCI-TK* gene for negative selection in gancyclovir, and the *pGK-neo* gene for positive selection in G418, subcloned into the *KpnI* and *HindIII* sites (respectively) of *pBSIISK* + (Stratagene). A genomic clone was isolated by screening a 129SVJ mouse lambda genomic library (Stratagene) with an *lrd* cDNA probe containing the first P-loop of the motor domain (Supp et al., 1997). A 6.3 kb *EcoRV* fragment was subcloned into the *BamHI* site of *pMJK-KO*, and a 0.8 kb *SpeI-XbaI* fragment was subcloned into the *XhoI* site (Fig. 4A). The construct was linearized by *NotI* digestion. Homologous recombination in ES cells and generation of gene targeted mice were performed using standard methods. Targeted ES cells and mice were genotyped using Southern blot analysis (data not shown) and PCR was used for confirmation (Fig. 4B). Primers used for PCR genotyping were: 3.7C, 5'-GGAAACATCTATAAAGGACTGGTG-3'; FAS-1, 5'-TGTTAGGACCCAAAGGTGGAAACAT-3'; and neo-1, 5'-CTTCC-TCGTGCTTTACGGTATCGCC-3'.

RT-PCR analysis of targeted *lrd* allele

RNA was prepared from entire heads and lungs of male mice by quick freezing in liquid nitrogen, grinding to a powder with a mortar and pestle and using RNazol (Tel-Test Inc.) according to recommended protocols, except that only 35 ml of RNazol was used for the pooled heads and lungs of two 7-week-old mice. The RNA was then further purified by phenol and chloroform extraction and ethanol

precipitation. An Oligotex mRNA Midi Kit (Qiagen) batch system was used to purify mRNA, which was reverse transcribed using the Superscript Choice System for cDNA Synthesis (BRL). Reverse transcripts were PCR amplified using Taq DNA polymerase (Qiagen) and the primers LRDj1 (5'-TCCGACACGAGTGGGAGGATT-CAAGGAAAC-3') and LRDj2 (5'-AGGAACACTGGGACAT-CATCAGTTACAATT-3'). Recommended Qiagen PCR buffer conditions, including 1× PCR buffer and 20% Q solution, were used. Samples were cycled at 66°C 1 minute, 72°C 3 minute, and 94°C for 1 minute, for 35 cycles and the products were resolved on 2% agarose gels.

Analysis of nodal cilia

Embryos were prepared for SEM by fixation for 90 minutes in 2.5% glutaraldehyde (EM) buffered with 0.1 M sodium cacodylate. SEM was performed according to standard protocols. Nodal cilia were visualized by light microscopy as previously described (Nonaka et al., 1998).

RESULTS

Complete *lrd* coding sequence confirms its classification as an axonemal dynein heavy chain gene

The full open reading frame of the *lrd* transcript has been cloned and sequenced. The *lrd* gene encodes a protein of 4,488 amino acids (Fig. 1A) with 60% overall amino acid sequence identity to the outer-arm β -axonemal dynein heavy chain of sea urchin, (Fig. 1B), compared with only 26% sequence identity with rat cytoplasmic dynein (Fig. 1C). The N-terminal one-third of the molecule is less conserved than the C-terminal two-thirds. This is consistent with the observation that cargo carrying and enzymatic functions that distinguish dynein family members from each other are located within the N-terminal region (Holzbaur and Vallee, 1994). The organization of the LRD motor domain is analogous to all other previously characterized dyneins. There are four centrally located P-loops spaced approximately 300 amino acids apart (Fig. 1A,E). The sequence TETTKDL, immediately following the first P-loop, further supports classification of LRD as a member of the axonemal-type dynein subclass. However, in contrast to several other axonemal-type dyneins (Kandl et al., 1995), no 5th P-loop is found in the N-terminal region of LRD. Two coiled-coil domains of 95 amino acids and 82 amino acids, separated by a 135 amino acid non-coiled region, are located 200 amino acids downstream of the 4th P-loop (Fig. 1D); this represents the likely LRD-microtubule binding site (Gee et al., 1997). RT-PCR identified an alternately spliced *lrd* mRNA that eliminates the third and least conserved P-loop, including amino acids 2521-2576. This smaller *lrd* message had an identical tissue distribution as full-length *lrd* (data not shown).

The *lrd* cDNA was also cloned and sequenced from *iv/iv* mice. Comparison of the coding sequence of the wild-type and *iv* alleles revealed only the previously reported difference, a glutamic acid to a lysine change in the conserved motor domain (Supp et al., 1997).

Expression of *lrd*

We previously showed that *lrd* expression at embryonic day 7.5 (E7.5) is limited to the node (Supp et al., 1997). The nature of this expression was examined further. Serial section in situ

hybridizations, using both frontal and transverse embryo orientations, showed expression in the node to be symmetric about the LR axis (data not shown). This symmetric distribution of *lrd* transcript was confirmed by whole-mount in situ hybridizations (Fig. 2A).

Expression studies with whole-mount embryo preparations revealed a striking pattern of *lrd* transcript distribution in E8.0-E8.5 embryos (0-7 somites). Of 146 embryos examined, 44% ($n=64$) showed *lrd* expression in the headfold region of the embryo, while 56% ($n=82$) showed no *lrd* expression in this region. Of the 64 embryos showing headfold *lrd* expression, 40 embryos had bilateral expression and 24 had asymmetric expression, with both left- or right-sided *lrd* expression patterns observed (Fig. 2B-D,F). There was no apparent correlation between developmental stage, as measured by somite count, and expression pattern. Sectioning revealed that this anterior expression was present in the gut endoderm and cephalic mesenchyme, and in the basal aspect of the overlying neurectoderm (Fig. 2E). In embryos with asymmetric expression, there was a sharp boundary between expressing and non-expressing cells at the midline of the embryo (Fig. 2E). Asymmetric expression in the anterior of the embryo is apparently a brief event, since the majority of embryos examined had either symmetric or no expression of *lrd* in this region (Fig. 2G).

Further analysis by serial section in situ hybridization showed continued *lrd* expression in E8.5 endoderm near the foregut/midgut junctional area (Fig. 3A,B). At this developmental stage, no signal was seen in the neural groove or developing heart. No *lrd* expression was detected in the notochord at any stage. At E9.5, *lrd* expression was observed in the endodermal lining of the midgut and hindgut (Fig. 3C). Expression in these regions was essentially undetectable by E10.5. At this stage, *lrd* expression appeared in the floorplate of the developing brain and neural tube, in a LR symmetrical pattern (Fig. 3D). At E10.5, floorplate expression was restricted to the anterior of the embryo, with no expression in the posterior neural tube (Fig. 3E). By E12.5, expression in the floorplate extended to the posterior of the neural tube (Fig. 3F). In addition, *lrd* expression was observed in mesenchymal cells ventral to the notochord (Fig. 3F, inset). This region does not appear to correspond to any particular embryonic structure. At E12.5 there was also strong expression in the epithelium lining the roof of the fourth ventricle of the brain (Fig. 3G). Expression in the developing limb was observed at E12.5 (Fig. 3H), and may correspond to regions of cartilage condensation. In newborn mice, expression was seen in several ciliated cell types, including the epithelial lining of the nasal cavity (Fig. 3I) and the ependymal lining of the third ventricle of the brain (Fig. 3J).

Deletion of the catalytic first P-loop of LRD by gene targeting

Previous studies suggested, but did not prove, the involvement of *lrd* in LR development. For example, while it was cloned from the *lgl* deletion, this region is large and encompasses many genes (Supp et al., 1996). In addition, the *lrd* gene in the *iv* mouse was found to carry a base difference that results in a coding change at a highly conserved position in the motor domain of the protein (Supp et al., 1997). Nevertheless, the original mouse stock on which the spontaneous *iv* mutation

A

MAAQEEGTVL	RLSPSEQEDE	EDEEAAAARR	VQRFALDPRV	CFLGGRLRQA	LRFPEETWGO	YLESDDHRQV	LGDFLESTGP	ASLVFSVATA	90
GRLSASPEIP	RDVVKHKLIVF	AKKMTENMGE	SDFSQTILFG	EIPRSLLTHV	TAFLDEILVP	VLSNKNHNTS	WSCFISQDVE	HTEVVMKNKM	180
HIFRGKMSRR	THLPIPTIAE	NIDLDQHLYV	TRPQSDERRI	LHAIESLTVK	WSHQIQEIIIG	KDSAHPLLSSG	LHPTPETELD	FTWHRHDLNK	270
CIYSQLQAPI	VLKMVKIIRT	RQSSYLPAK	GIFTTVENAL	LEAQDVELHL	RPLRRHHIHL	QEAFFPQTRI	LIAPLLHTIC	LIWSHSHFNK	360
TPARVIVLLQ	EFCNLFIDQA	RAYLSPEDLL	KGEIEDALEK	VQVAISVLKT	FQNSFFKYRK	GLTSYFTRNT	EQRPWDFQSH	LVFGRFNKFL	450
DRLVKIEDMF	VTILEFEKLE	RLEFGGSKGA	VLNAQIHSTS	EEFIECKVVF	QQSTYDPSDC	DDMEFESDYF	KFKSRTLLDFD	RRLGTLLECG	540
LSNCSGLESA	FKLLTIFGNF	LEKPVVMEFM	SPHYSTLLNM	FNAELDVCKQ	LYDEHMKQIE	HGHEILNKNM	PFTSGNIKWA	RMLLERLQMF	630
WSNFTSLHYL	FPDSDPEAAV	CQKYAEMTTL	LDQFESHYS	EWRRNVDETC	EFNLNQPLVK	FSPINGLLSV	NFDPKLVAVL	REVKYLLMLK	720
EVHRTRFSFR	HFPEKDIILK	YIGNLELLVQ	GYNKLIKQTL	EVEYPLIEDE	LGAIDEQLRV	AATWLTWQDD	FWVYMERVQV	ATAELECVRV	810
QTQSNMLTIQ	QTMQAWAEPW	LLPRRETRE	AALTLDDKGD	LFAKKYKLIR	EDGCKIHNLV	EENRKLFRAD	PSLDSWKIYV	EFIDDIVVVG	900
FFQAAILHDL	FFLRNTEKQL	KPTPPFQAQM	LLMPEEIVFK	PPELEKAGDG	FYDLVEEMLC	GSFRVSAQMG	RVAALHDIAI	YQNDMDNMLG	990
LAEVRQEIFM	RVADVINKVL	EFRILWRPRL	NLWVDDRVEI	LRQFLLYGHA	VPSEEMDAPA	SEDILQPPTL	EQFQEKIDIV	EALYIQMSKF	1080
DDFRVFNWSF	KVDMRPFKLS	LLNVIKKWSW	MFQEHLLRFV	VDSLSELQGF	IKQTNAGLQR	QLCEGDHDLG	VDIMGHLLAV	RSRQRATDEL	1170
FEPLKETIML	LESYQKMPKE	QVYAQLEELP	ERWETTKKIA	AMVRHEVSLP	QNAEVTLLRK	KCILFDEKQA	EFRRFRSRYA	PLGFKAENPY	1260
AVLDKANQEL	EALEEEMEQM	QNSARLFEVA	LPEYKQMKQC	RQEIRLLKGL	WDVI IYVRS	IDNWTETQWR	QINVEQMDLE	LRRFAKEIWS	1350
LDKAVRVWDA	YSGLEGTVKD	MTTSLRAIAE	LQNPALDRRH	WQQLMKAIGV	RFSINDSTTL	SDLLAVQLHR	VEDDVRDIVD	QAVKELGTGK	1440
VITDVSHSTE	ALEFSYEAHH	RTGTPLLKSD	EQLFETLEHN	QVQLQSLLOS	KYVEYFIEQV	LSWQNLNVA	DAVIFTWQMV	QRTWSHLESI	1530
FVCSIEDIRVQ	LVEDARRFDK	VDAAEFKELMF	ETAKVKNVLE	ATCRPLHYEK	LKDPQHRLSL	CEKALAEYLE	TKRVTFPRFY	FISSADLLDI	1620
LKSQAQPKQV	THHLVKLFDS	ISDLQFEDNL	DVSTHKAQVM	FDSKHEYYVFP	QAGCECIGHV	ESWLLQLEQT	MKDTVRLAIT	EAITAYEEKP	1710
RELWIFDFPA	QVALTGIAFS	WTTDVGIAFS	RLEEGYETAL	KDFHKQIQSQ	LNTLITLTLG	ELSPGDRQKV	MTICTIDVHA	RDVVAKLIQS	1800
KVVSPhaftw	LSQLRHWEDE	SRKHCVVNIC	DAHFOYFYEY	LGNSPRLVIT	PLTDRCYITL	TQSLHLTMSG	<u>APAGPACTGK</u>	<u>TETTKDLGRA</u>	1890
LGMVYVYFNC	SEQMDYRSIG	NIYKGLVOTG	AMGCFDEFNR	IAYEVLVSVA	VQVKMIHDAI	RNGRKRFFVL	GETIPLKPSV	GIFTITLNPGE	1980
AGRTELPELN	KALFRPCAMV	APDTELICEI	MLVAEGFVDA	RSLRALKFISL	YTLCEELLSQ	QDHYDWGLRA	TKSVLVVAGS	LKRGGDKRPE	2070
DQVLMRALRD	FNMPKIVTDD	VPVFLGLVSD	LFPALDVPQR	RKPHFQMYK	QCTLELRLQP	EESFILKVVQ	LEELLAVRHS	VFVV <u>ENAGTC</u>	2160
<u>KSKILRLTNR</u>	TVVNKMQKPV	WSDLNPKAVT	TDELPGFIHH	ATREWKGDLF	SSILREQANL	THDGPTWIVL	DGDDIDPLWIE	SLNTVMDDNK	2250
VLTLASNERV	ALKPMSRLLF	ETHHLRTATP	ATVSRAGILY	VNPQDLGWNP	YVASWIDRRR	HQSEKANLTI	LFDKYIPVCL	EKLRTSFKAI	2340
TSVPESLIVQ	TICTLLECLL	TPENIPDPSF	KETYEVYFAF	ACVWTFPGTL	LKDQLSDYQA	DFSRWVKHEM	KAVKFPSSQT	IFDYLDHKT	2430
KKFLPWTDKV	PQFSMDADAP	LKTVLVHTPE	TTRLRYFTEL	LLCKGKPIML	VGNAGVGKTV	FLSNTLASLS	ENYIVSCVPF	NYTTSAAALQ	2520
RILEKPLEKK	AGRNYGPKKN	<u>KKLVYFIDDL</u>	<u>NMPEVDLYGT</u>	<u>VOPHALLRH</u>	<u>IDYGHYWRDH</u>	KIMLKEIRNC	QYVACMNPMF	GSFTVNPRLQ	2610
RHFTVFAFNF	PSLDALTTIY	QGI ² FSY ¹ LQ ²	QAF ² CP ¹ SV ¹ LQ ²	GPSLIQ ² ATIA	FPHQMAESFV	PTAIKFHYNF	NLRDLSNIFQ	GILFASPECL	2700
KSLEDLARLW	LHETSRYYGD	RLIDTNDFDL	FQKMLETAH	KYFKGVDAANA	LLRQPLVYCH	FASGGEDPCY	MPVKDWEGLK	AVLMEMVDNY	2790
NELHSAMHLV	LFEDAMQVHC	RISRILRIPQ	GHALLI ¹ GVGG	SGK ² OSLSRLA	AYICSLVDFQ	ITLTEGYGAQ	ELRVDLANLY	VRTGAKNMP	2880
VFLLTDAHLV	DESFVLVIND	LLASGDIPDL	FSDEDMDKII	SGIRNEVRGL	GLVDSRENCV	AFFLARVRQV	LKMVFCFSPV	GHTLRVRARK	2970
FPAIVNCTAI	DWFHEWPEEA	LVSVSRRFIE	EIEGLEPQHK	DSISLPMMAH	HTSVKEVSAW	YYQNERRYNY	TPRSFLEQI	SLFKSLLKKK	3060
REEVKQKQEH	LGNGIQKLQT	TASQVGNLKS	RLASQEAELQ	LRNLDAEALI	TKIGLQTEKV	SREKAIADAE	ERKVAAIQTE	ASQKQRECEA	3150
DLLKAEPALV	AAKDALNTLN	RVNLTTELKTF	PNPPNAVTVN	TAAMVLLAP	RGRVPKDRSW	KAAKIFMGKV	DDFLQALIN	DKEHIPENCL	3240
KVVNEQYLKD	PEFNPNLIRT	KSPAAAGLCA	WVINIIRFYE	VYCDVEPKRQ	ALAAQTNLDDA	AAATEKLEAVR	RKLVDLHDNL	SRLTASFPEKA	3330
TAEKVRQCEE	VNQTKNTIDL	ANKLVSELES	EKIRWQGSIK	SFETQEKTLK	GDVLLTAAVF	SYIGSFTRQY	RQELVDCKWI	PFLQKQVSIIP	3420
IAEGLDLIAM	LTDATIAATW	NNEGLPSDRM	STENATILTH	CERWPLMIDP	QQQGLKWKIN	KYGPDLKVTH	LGQKGFINTI	ETALAFGDVI	3510
LIENKLETVD	PVLGPLLGRN	TTKKGKFI RI	GDKCEFNKN	FRLLILHTKLA	NPHYKPELQA	QTLLNFTVT	EDGLEGQLLA	EVVSIERPDL	3600
ERLKLVLTKQ	QNDFKIELRQ	LEDDLLRLS	AAEGSFLDDT	DLVERLETTK	ATAAEIEHKV	TEARENERKI	NETRECYRPV	AARASLYFV	3690
ISDLRRINPV	YQFSLKAFNT	LFHRAIEQAD	KVEDTQERIC	ALIESITTHAT	FLYASQALFE	RDKLTFLSQM	AFQILLRRNE	IHPLELDPLL	3780
RFTVEHTYSS	PVDFLTAQSW	SAVKAVALME	EFRGLDRDVE	GSAKQPKVK	ESECEPEKEL	PQEWKKSLSI	QKLIILRAVR	PRDMTYALRN	3870
FVEKLGAKY	VERTRLDLGK	AFEESSPSTP	VFFILSPGVD	ALKDLVEVLG	RLGFTIDSQK	FHNVS LGQOQ	ELVAFDQMLE	AAAGGYHFLK	3960
QNVHLVAKLV	GTLEKLLLEK	SQGSHRDYRV	FLSAETVPSQ	HEPIIPQGLK	ENSIKITNEP	PTGMLANLHA	ALYNFDQMTL	EMCSKQDPEF	4050
SILFSLCYFH	ACVAGRLRFQ	PQGWRSYPF	SPGDLTICTN	ILYNYLEANP	NVPWEDLRYL	FGEIMYGGHI	TDAWRKLCR	VYLEEFMNP	4140
LIEDEVMLAP	GFAAPPYSYD	SGYHQYIEDT	LPPESPALYG	LHPNAEIELL	NVTSNTLFRP	LLEMQRNAV	SQELGGQSTE	DVKNILDDI	4230
LERLPEEFNM	ABELMQKNPR	SPYVLVCFQE	CERNMVLIRE	IRVSLQHLDD	GLKGLTSLP	DVETQLSALS	YDRVPDTWNL	LALPSTYGLA	4320
QWFNDLLRC	RELDWTQDL	TLPAVWVLSG	FFNPQSFLTA	IMQTMARKNE	WPLDRMCLTI	DVTKTKKEDY	GHPREGAYL	HGLHLEGARW	4410
DIQSGALVDA	RLKELTSMMP	VIFAKAVPVD	RQEKIHAHEC	PVYKTKARGE	TYVWTFRLRS	KDRIAKWVLA	GVALLEA	4488	

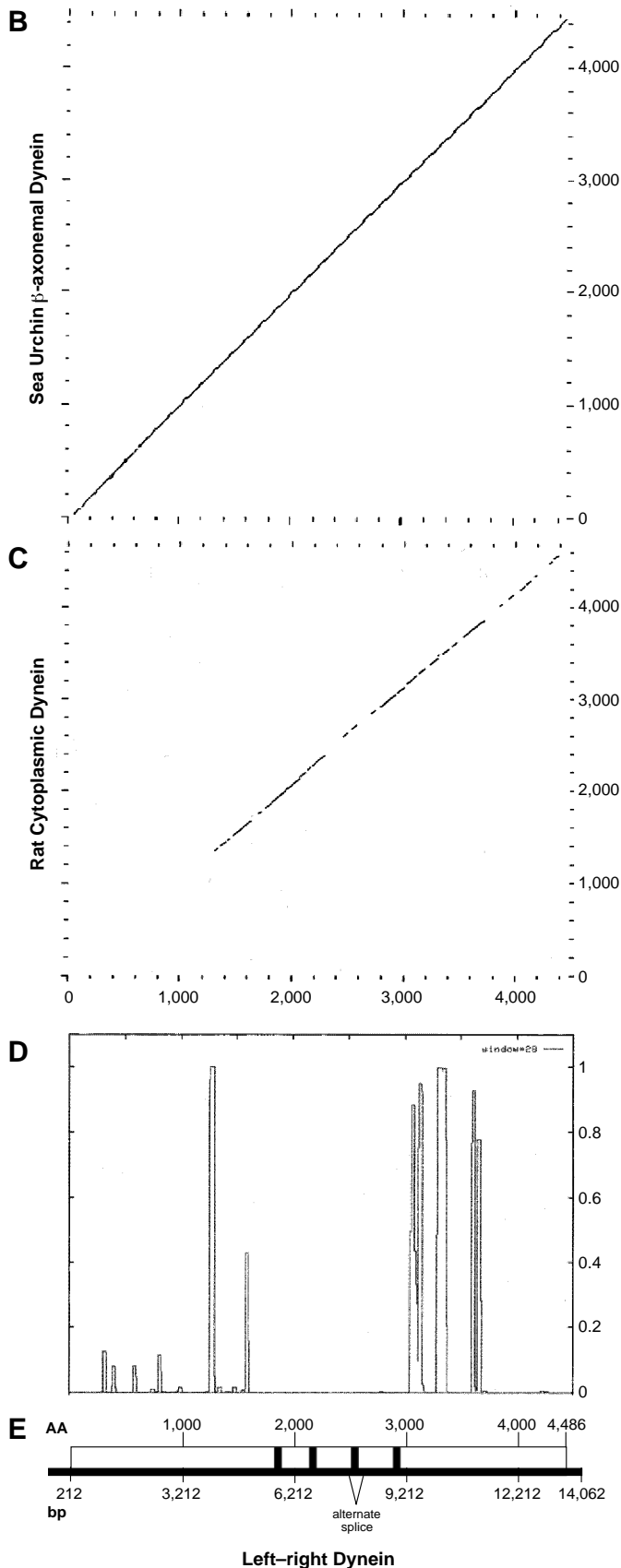
Fig. 1. Sequence of LRD and homology with sea urchin axonemal dynein β heavy chain. (A) LRD amino acid sequence. The four P-loops are highlighted. Thin underline, exons deleted in targeted *lrđ* mutation. Thick underline, exon missing in alternately spliced form of *lrđ*.

(B-E) Analysis of LRD amino acid sequence; amino acid residues in B-D are aligned with the map shown in E. (B,C) Comparisons of LRD amino acid sequence with sea urchin b-axonemal dynein and rat cytoplasmic dynein. The comparisons were done using the Compare program (GCG, University of Wisconsin), using a window of 50 and a stringency of 40. Note the higher degree of overall homology of LRD with sea urchin b-axonemal dynein (B) compared with rat cytoplasmic dynein (C). (D) Coiled-coil analysis of LRD amino acid sequence using the COILS program. Note the coiled-coil structures predicted immediately C-terminal to the 4th P-loop. (E) Representation of the *lrđ* mRNA and amino acid sequence aligned with B-D. Thick horizontal line, sequenced mRNA. Open rectangles, translated regions; shaded boxes, P-loops. Accession number AF183144.

arose is no longer available for comparison, so it remained possible that this base change represented a polymorphism. Finally, expression of *lrđ* was found in the node of the embryo (Supp et al., 1997), which again suggested a role in LR axis formation, but did not prove it. To confirm the role of *lrđ* in LR specification, to determine if *lrđ* is required for limb or gut development and to test models for the mechanism of *lrđ* function, a targeted mutation was generated.

Several studies have indicated that, of the multiple P-loop motifs in the motor domain of dyneins, only the first P-loop is actually involved in ATP hydrolysis (Gibbons et al., 1991; Gee

et al., 1997). To generate a protein unable to catalyze ATP hydrolysis and therefore without motor activity, we deleted two exons of the *lrđ* gene that encompass the first P-loop (Fig. 4A) by homologous recombination in ES cells, and used these cells to generate heterozygous mice. Mice were genotyped by PCR (Fig. 4B). RT-PCR analysis of heterozygous mice showed the expected products for wild-type and targeted alleles (Fig. 5). The targeting vector was designed such that mRNA splicing would generate a transcript with the correct reading frame that lacked the first P-loop. To confirm correct processing, mutant *lrđ* RT-PCR products were subcloned and sequenced. Six of



seven clones analyzed showed precisely correct splicing around the deleted exons, using the predicted splice donor and acceptor sequences of the flanking exons. The seventh clone skipped the exon immediately 3' of the deleted exons but also failed to generate a frameshift mutation. Taken together, the RT-PCR studies strongly suggest that a significant fraction of *lrd* transcripts from the knockout allele were properly processed around the two deleted exons to retain the reading frame.

Randomized LR development in targeted *lrd/lrd* mutants

Mice heterozygous for the *lrd* targeted mutation were overtly normal. Of an initial set of 85 progeny of matings between *lrd* heterozygotes which were genotyped at weaning, 16 mice (19%) were found to be *lrd*^{-/-} homozygotes, 50 (59%) were heterozygotes and 19 (22%) were wild type. This is not statistically different from the expected 1:2:1 ratio, indicating an absence of embryonic lethality. Gross examination of neonates revealed that approximately half of homozygous mutants had inverted right-sided stomachs. No phenotype was detected in heterozygotes. To better define the LR phenotype, 31 *lrd* homozygous mutant mice were dissected and examined for laterality of the lungs, heart, stomach, liver and spleen. Fifteen had normal laterality for these organs, with a single-lobed lung on the left and a multiple-lobed lung on the right, heart apex on the left, normal liver lobe pattern, and stomach and spleen on the left. Twelve animals showed a complete reversal of positioning of these organs. In addition, two animals showed heterotaxia, a discordant positioning of individual organs within the same animal, with the heart and liver normal but the stomach and spleen reversed. One of these had normal lungs and the other had an isomerism, with both left and right lungs showing a single-lobed (left-sided) pattern. The remaining two animals had left lung isomerism with one having otherwise normal situs, and other having reversed situs. These findings are similar to those obtained from the analysis of liveborn *iv* mutant mice.

Gross malformations of the limbs and face, such as those seen in *lgl/lgl* mutant mice (McNeish et al., 1990), were not observed in the targeted *lrd/lrd* homozygous mutants. Skeletal staining of *lrd/lrd* mutants was performed to look for more subtle malformations, and none were found.

Nodal cilia of the *lrd* mutants are present but immotile

Adult ciliary function is normal in *lrd* mutants. Male *lrd/lrd* mice are fertile, indicating the presence of motile, functioning sperm. In addition, tracheal cilia are present and beat (data not shown). The absence of defects in sperm tails and tracheal cilia was previously reported for the *iv/iv* mutant mice (Handel and Kennedy, 1984).

The nodes of E7.5 *lrd/lrd* and *iv/iv* mutants were examined by scanning electron microscopy, and normal monocilia were observed (Fig. 6). The cilia in these mutant embryos were the same size and distribution as seen in wild-type embryos. The nodal cilia of freshly dissected embryos were also examined by light microscopy. It was observed that the wild-type cilia of the node exhibited a 'vortical' motion as reported by Nonaka et al. (1998). Of interest, the *lrd* mutant cilia were

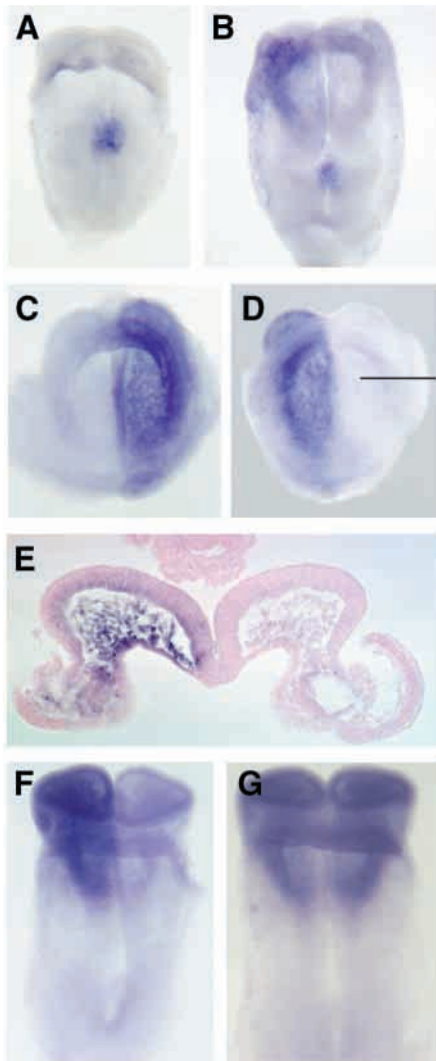


Fig. 2. Expression of *lrd* in E8 and E8.5 embryos localized by whole-mount in situ hybridization. All are ventral views, so the right side of the embryo is to the left of the figure. (A) Early E8 embryo, showing symmetric *lrd* expression in the node. (B) Slightly older E8 embryo showing *lrd* expression in the node and in the right anterior. (C,D) E8.25 embryos showing strong anterior asymmetric expression on the left (C), or on the right (D). The posterior of both embryos is curled away and not visible. (E) Transverse section through the anterior region of the embryo in D at the level indicated by the line. Expression is strongest in the endoderm and head mesenchyme but is also apparent in the overlying neuroectoderm. (F) E8.5 embryo showing strong asymmetric anterior expression. (G) E8.5 embryo with symmetric anterior expression.

rigid and immotile (<http://genome.chmcc.org/cilia/> and <http://www.biologists.com/Development/movies/dev3019.html>).

DISCUSSION

lrd is required only for LR development

Previous results, including the expression of *lrd* in the node and the presence of a mis-sense base change in the *lrd* gene of the *iv* mouse strain, strongly suggested but did not prove *lrd*

function in LR determination. The randomized laterality observed in *lrd* targeted mice demonstrates conclusively that *lrd* is required for normal LR development and confirms that the *iv* and *lrd* genes are the same. The three mutant alleles of *lrd* can therefore now be referred to as *lrd^{iv}*, *lrd^{sl}* and *lrd^{ΔP1}*.

Loss of LRD motor function appears to only affect LR development. In this regard, the *lrd* mutation is unique among those affecting LR asymmetries. Mutations of *lefty-1* (Meno et al., 1998), *kif3A* (Marszalet et al., 1999; Takeda et al., 1999), *kif3B* (Nonaka et al., 1998), *Ft* (Heymer et al., 1997), *inv* (Yokoyama et al., 1993), *Mgat* (Metzler et al., 1994; L. A. L. and M. R. K., unpublished), *SIL* (Izraeli et al., 1999), and *nt* (Melloy et al., 1998) all result in prenatal or postnatal lethality that is often accompanied by severe midline and/or anteroposterior defects. The expression of *lrd* in the developing limbs and the truncated hindlimbs in mice homozygous for the *lgl* deletion had suggested a possible function for *lrd* in limb development. It remains possible that the *lrd* transcripts from the targeted *lrd^{ΔP1}* allele retain function in limb development but not LR axis formation, resulting in a less severe phenotype than the *lrd^{sl}* allele, which has a deletion of the entire *lrd* gene. A more likely explanation is that additional gene(s) deleted by the *lgl* transgene insertional mutation are responsible for the *lgl/lgl* mutant limb defects.

Targeted *lrd^{ΔP1}* homozygous mutant mice did not exhibit the poor reproductive performance or the relatively high resorption rate and resultant small litter size observed with mice of the *lrd^{iv}* strain (Brown et al., 1989). This may represent a modification of the phenotype due to genetic background differences, or it may be due to subtle differences between the targeted *lrd^{ΔP1}* allele and the spontaneous *lrd^{iv}* mutation.

Motile tracheal cilia were present in *lrd^{ΔP1}* mutant mice, and males were fertile, indicating normal sperm motility. In contrast, human males with Kartagener syndrome, which display randomized visceral asymmetry, are generally sterile with immotile sperm and suffer respiratory tract infections due to immotile tracheal cilia (Afzelius, 1976). The results of the *lrd* gene targeting in this report indicate that a dynein functional disturbance could be directly responsible for the laterality defects of Kartagener patients. The differences in the *lrd* mutant and Kartagener phenotypes, however, suggests the involvement of distinct dynein genes, or dramatically different mutant alleles.

lrd may be involved in both establishment and maintenance of LR asymmetry

Expression of *lrd* in the node at the late primitive streak/early head fold stage is consistent with a role in LR determination. Other genes implicated in LR development are also expressed in and around the node at these stages, including *nodal* (Lowe et al., 1996; Collignon et al., 1996), *lefty* (Meno et al., 1996), *HNF3β* (Collignon et al., 1996; Dufort et al., 1998), *Shh* (Echelard et al., 1993; Izraeli et al., 1999) and *kif3B* (Nonaka et al., 1998). The striking pattern of *lrd* expression observed in slightly older embryos is altogether novel. Roughly 50% of embryos at this stage (0-5 somites) showed expression of *lrd* in all three germ layers, at the anterior of the embryo in the region of the erupting head folds. Some embryos displayed left-sided expression, some showed right-sided expression and some had bilateral expression. This period of expression, especially the asymmetric expression, is apparently fleeting

since it is observed only in a fraction of embryos analyzed. Direct correlation between sidedness of *lrd* expression and somite number was not observed. Overlapping this period, but beginning slightly later, there is lateral asymmetric gene expression of *nodal*, *lefty-2* and *Pitx2* in the left lateral plate mesoderm and *SnR* in the right lateral plate mesoderm. *lrd* expression, however, is not in the lateral plate, but is more anterior, dorsal to the precardiac region. It is tempting to speculate that this transient asymmetric domain of *lrd* expression functions in the transfer of LR patterning information from the midline node to influence the rightward looping of the heart tube. This *lrd* expression also suggests a possible role in the establishment of anterior central nervous system asymmetries.

The only defect detected in the *lrd*^{ΔPI}/*lrd*^{ΔPI} mutant gut was randomized laterality. This suggests that the observed *lrd* expression in the developing gut may be involved in LR specification. Although the gut tube begins to close at E8.5, the gut does not initiate handed asymmetric coiling until after mid-gestation. Expression of *lrd* in the gut endoderm is only found up to E9.5, suggesting that *lrd* may not directly function in the lateralization of the gut, but rather acts through an indirect mechanism as proposed above for heart looping.

Expression of *lrd* in E10.5-12.5 embryos was found in the floorplate of the neural tube.

This midline structure has been implicated in LR specification, although at earlier stages of embryonic development. For example, extirpation of the notochord, hypochord and floorplate from *Xenopus* embryos, at stages when the neural tube is still open, randomizes LR asymmetries and disrupts the normal left-sided expression of *Xnr-1* (Lohr et al., 1997). Furthermore, several mutations in zebrafish (Danos and Yost, 1996; Goldstein et al., 1998) causing midline defects and mutations in mice causing defects in either the node, notochord

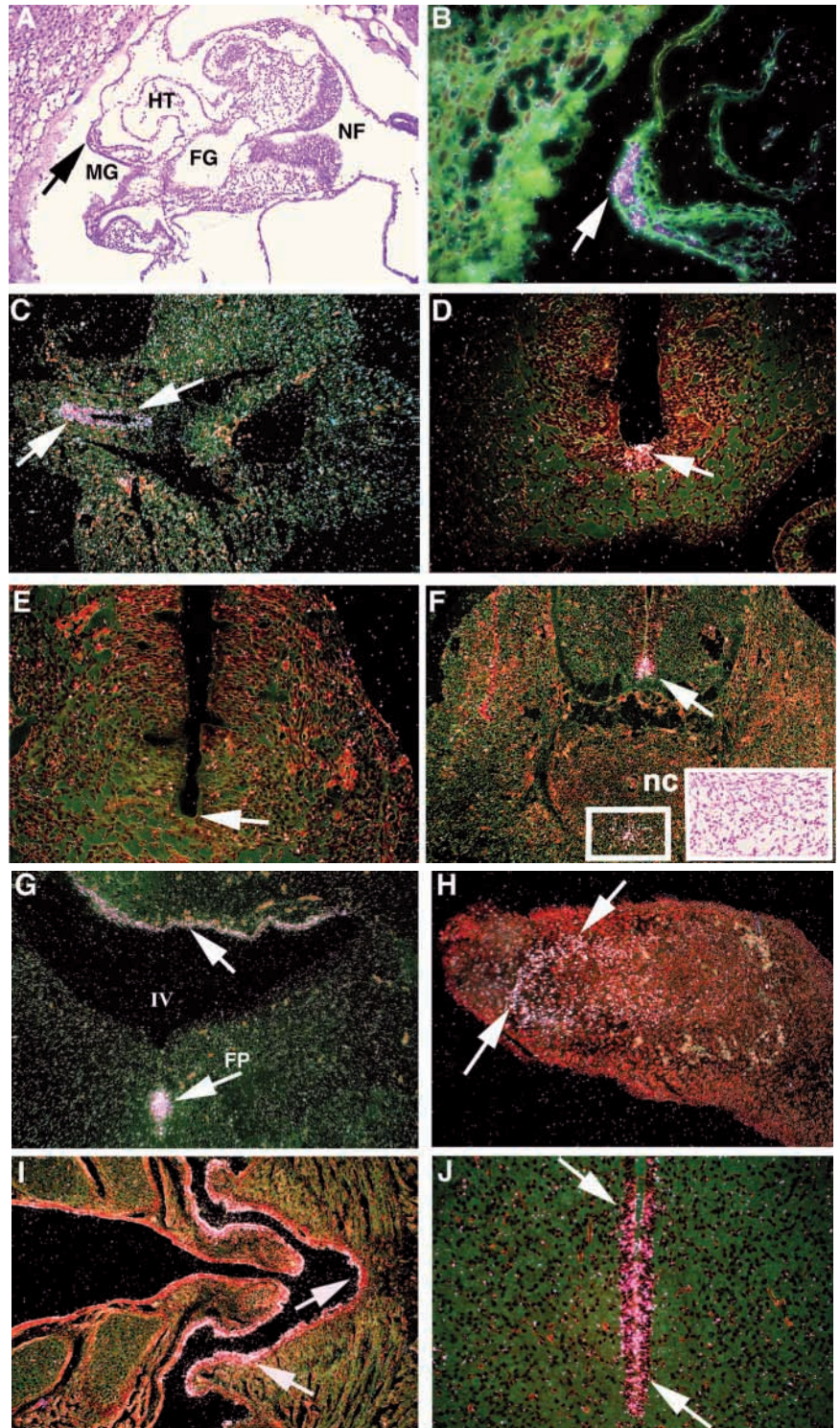


Fig. 3. Expression of *lrd* localized by serial section in situ hybridizations. (A-J) Hybridization to antisense *lrd* riboprobe; no signal was detected with a sense control probe (not shown). (A) Bright-field transverse section of an E8.5 embryo, showing the locations of the heart tube (HT), midgut region (MG), foregut (FG) and neural fold (NF). (B) Dark-field, magnification of A, showing *lrd* expression the endoderm adjacent to developing midgut (arrow). (C) E9.5 embryo showing expression in the hindgut (arrows). (D) Transverse section through the abdominal region of an E10.5 embryo showing expression in the floor plate of the anterior neural tube (arrow). (E) The posterior neural tube shows no hybridization (arrow). (F) Transverse section through the abdominal region of an E12.5 embryo showing expression in the floorplate of the neural tube (arrow) and a region of cells (boxed) ventral to the notochord (nc). These midline cells are distinguished only by their mesenchymal character (insert, bright field). (G) Expression of *lrd* in E12.5 brain (arrows), in the epithelium lining the fourth ventricle (IV) and in the floorplate (FP). (H) *lrd* expression in mesenchyme of the limb of an E12.5 embryo (arrows). (I, J) Transverse sections through the head of a newborn mouse showing *lrd* expression (arrows) in the ciliated epithelium lining of the nasal cavity (I) and the ependymal lining of the third ventricle of the brain (J).

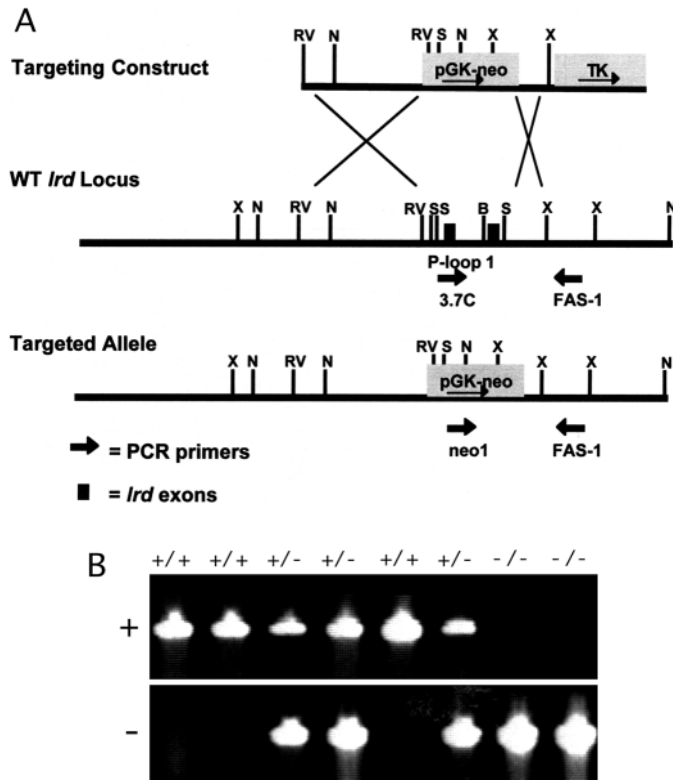


Fig. 4. *lrd* gene targeting. (A) Gene targeting construct (top), wild-type *lrd* locus (middle) and structure of targeted allele (bottom). Two exons of the wild-type *lrd* sequence (black boxes), including the exon encoding the first P-loop, were replaced by the selectable *neo* gene. Shown are the locations of PCR primers (not drawn to scale) used for genotyping. (B) PCR genotyping of mice. Targeted allele yields a PCR product with *neo1* and FAS-1 primers. The wild-type allele yields a PCR product with the 3.7C and FAS-1 primers. Note, the FAS-1 primer flanks the region of homology between the targeting construct and the endogenous locus. Abbreviations: RV, *EcoRV*; N, *NcoI*; X, *XhoI*; S, *SpeI*; B, *BglII*.

or neural tube (Metzler et al., 1994; Heymer et al., 1997; Melloy et al., 1998; King et al., 1998; Izraeli et al., 1999; Takeda et al., 1999) lead to randomization of LR asymmetries. In addition, mutation of *lefty-1*, which is expressed asymmetrically in the floorplate, results in isomerisms (Meno et al., 1998). The likely role of these midline structures including the floorplate, early in the development of the LR axis, is either in signaling (Lohr et al., 1997; Izraeli et al., 1999) or as a midline barrier (Meno et al., 1998; Vogan and Tabin, 1999). Expression of *lrd* in the floorplate at later stages, after morphological asymmetries have been established, may indicate a heretofore unrealized role for the floorplate in maintaining laterality or in patterning later occurring asymmetries.

Models for *lrd* function in LR development

Several models for LR axis determination have been proposed (Brown and Wolpert, 1990; Klar, 1994; Srivastava, 1997; Levin and Mercola, 1998; Nonaka et al., 1998; Vogan and Tabin, 1999). These models can be grouped into two categories: those that require LRD motive force and those that do not. One model, based on the binding of a Gli-family transcription factor

Fig. 5. Molecular analysis of RNA splicing of *lrd* targeted allele. RT-PCR analysis of *+lrd* RNA was performed using primers flanking the targeted deletion, and resulted in an 844 bp product from the wild-type allele and a 547 bp product from the mutant allele (lanes 1,2). Doubling of the input RT (lane 2) product resulted in an approximate doubling of the PCR product bands, suggesting that the reaction conditions were within the linear range. M, ϕ X174 RF DNA/*HaeIII* molecular weight standard.

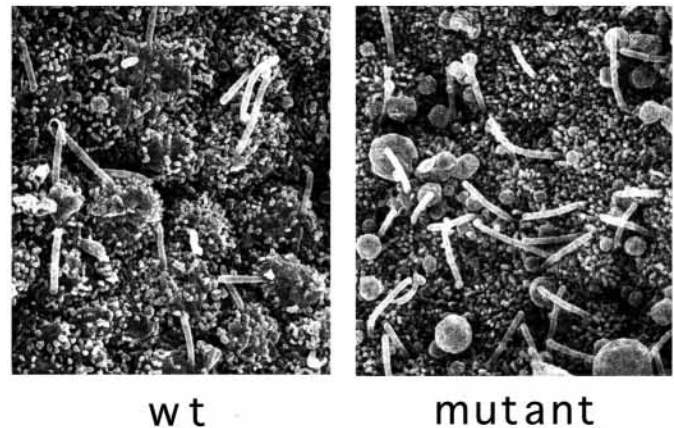
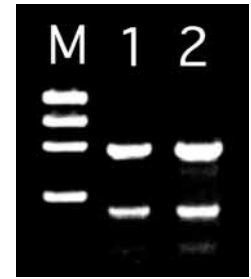


Fig. 6. Monocilia on the nodes of E7.5 wild-type and *lrd* mutant embryos. Scanning electron micrographs of embryonic nodes showing the presence of cilia on the ventral cell surfaces. Wild type is shown on the left and mutant (homozygous for targeted *lrd* allele) on the right. Embryos homozygous for the *iv* spontaneous mutant allele of *lrd* also had node cilia that appeared indistinguishable from wild type (data not shown). The cilia are approximately 1.5 μ m in length.

by the kinesin-like molecule *costal2* in *Drosophila*, invokes a cytoplasmic anchoring function for LRD (Srivastava, 1997). According to this model, LRD is held in the cytoplasm by its binding to microtubules, and LRD in turn binds to a transcription factor, perhaps *Zic3*, a transcription factor mutated in X-linked heterotaxias in humans (Gebbia et al., 1997). Binding of LRD to *Zic3* would hold it in the cytoplasm, until a signal (Shh for the *costal2*-Gli pathway in *Drosophila*) triggers its release. Upon release the transcription factor would translocate to the nucleus and modulate gene expression patterns. According to this model, LRD would respond to an asymmetric signal and represent a component of a signal transduction pathway. This model requires LRD binding to microtubules and the putative transcription factor, but not motive force. Srivastava (1997) suggested that the mis-sense mutation in the motor domain encoding region of the *lrd^{iv}* allele perturbed transcription factor binding and hence disrupted LR determination function. The *lrd^{ΔP1}* allele carries a mutation that alters a distinct domain of the LRD protein that is also required for motor activity. It is quite unlikely that both of these mutations would eliminate the proposed transcription factor binding domain, and neither alters the known microtubule

binding domain. The results suggest, therefore, that LRD must have motor activity to perform normal LR axis specification.

Other models have been proposed that require LRD motive force for LR specification. For example, an attractive model originally proposed by Brown and Wolpert (1990) and recently updated by Levin and Mercola (1998) proposes a handed asymmetric molecule, represented by the letter 'F', aligning in a specific fashion with respect to the AP and DV axes and thereby orienting the LR axis. In this model, LR asymmetries would result from an asymmetric movement of molecules or cellular components directed by the 'F' molecule. The results presented here support this model and suggest that the function of the hypothetical 'F' molecule is supplied by node monocilia.

The 'nodal flow' model also requires LRD motive force. It was observed that, in wild-type embryos, the monocilia of the node undergo 'vortical' motion that results in a leftward 'nodal flow' of extraembryonic fluid (Nonaka et al., 1998). This could hypothetically create a LR asymmetry of a soluble morphogen in the extracellular fluid of the node (Nonaka et al., 1998). In this report, we have shown, as was predicted by others (Nonaka et al., 1998; Vogan and Tabin, 1999), that LRD motor function is required for normal motility of the node monocilia.

The phenotypes of mice with targeted mutations in the *kif3A* and *kif3B* genes support but do not prove the 'nodal flow' model. These mice have absent node monocilia and defective LR development (Marszalek et al., 1999; Takeda et al., 1999; Nonaka et al., 1998). The KIF3A and KIF3B proteins, together with the non-motor KAP3 protein, form the heterotrimeric kinesin complex. This complex functions as a plus-end directed microtubule motor, and the heterotrimeric kinesin complex has been shown to be required for ciliary assembly in sea urchin and *Chlamydomonas* (Morris and Scholey, 1999). Gene targeting demonstrated the requirement for KIF3A and KIF3B in assembly of node monocilia in mice and implicated these cilia in the development of LR asymmetry. Nevertheless, monocilia are unusual in structure and have been proposed to have multiple functions in addition to motility. Monocilia have a 9+0 microtubule organization instead of the more common 9+2. Such cilia have been generally considered non-motile and have been suggested to have a sensory function, or to indicate cell polarity (Wheatley et al., 1996), or to play a midline barrier role (Vogan and Tabin, 1999). In the *kif3A/B* mutants, the node monocilia are entirely absent, removing all ciliary function, not just motility. In *lrd* mutants, the node monocilia are present but immotile, presumably more precisely perturbing nodal flow.

The *lrd* and *kif3A/B* mutations perturb nodal cilia and LR development, but the LR phenotypes are not identical. In *kif3B* mutants, embryonic turning is not randomized as in *lrd*^{ΔP1} or *lrd*^{iv} mutants. Instead most *kif3B*^{-/-} mice fail to turn altogether and die by E10. More interesting, in *kif3B* mutants, expression of *lefty* is absent or bilateral (symmetric), in contrast to the randomly asymmetric pattern observed in *lrd*^{iv} mutants. Mutants lacking *kif3A* also die by E10 and display neural tube degeneration and mesodermal and caudal dysgenesis in addition to absence of node cilia and LR randomization (Marszalek et al., 1999; Takeda et al., 1999). The different developmental defects can be at least partly explained by much broader developmental roles for *kif3A* and *kif3B*. In striking contrast to the kinesin mutations, there are only two discernable abnormalities in *lrd*^{ΔP1} mutant mice: the node cilia in E7.5 embryos are rigid rods that do not exhibit normal

vortical motion, and there is random development of LR asymmetry, without other developmental defects. The observed 'rigor' state of the *lrd*^{ΔP1} mutant cilia is consistent with the report that cytoplasmic dynein with a defective P-loop irreversibly binds microtubules (Gee et al., 1997). The distinct LR phenotypes argue that the *lrd* and *kif3A/kif3B* mutations do not both work exclusively through identical blocks of nodal flow.

The data presented here strongly support the hypothesis that node cilia are motile and that it is motility of these cilia that is required to generate left-right asymmetry. Thus, 'F' is the node monocilium: a chiral macromolecular structure that is oriented relative to the existing AP and DV axes. This structure can convert its inherent chirality to organismal handedness by directional movement of a soluble substance at the node powered by the left-right dynein motor.

The authors wish to thank John Dunlop and Kyle Vogan for scanning electron micrographs, Diane Bodenmiller, Jen Lachey, Pam Groen, Kathy Saalfeld and Lisa Artmayer for technical support, and Alicia Emley for photographic assistance. Also, special thanks to the Webmaster, Bruce Aronow, for creating the web movies of wild-type and mutant cilia. This work was supported by NIH grants HD24517 to S. S. P., HD36439-01 to M. B., HD07200 to D. M. S., AHA (OH-WV Affiliate) grant SW-96-43-S to D. P. W. and a grant from the Hood foundation to M. B.

REFERENCES

- Afzelius, B. A. (1976). A human syndrome caused by immotile cilia. *Science* **193**, 317-319.
- Brown, N. A., Hoyle, C. I., McCarthy, A. and Wolpert, L. (1989). The development of asymmetry: the sidedness of drug-induced limb abnormalities is reversed in *situs inversus* mice. *Development* **107**, 637-642.
- Brown, N. A. and Wolpert, L. (1990). The development of handedness in left/right asymmetry. *Development* **109**, 1-9.
- Campione, M., Steinbeisser, H., Schweickert, A., Deissler, K., van Bebber, F., Lowe, L. A., Nowotshcin S., Viebahn, C., Hafter, P., Kuehn, M. R. and Blum, M. (1999). The homeobox gene *Pitx2*: mediator of asymmetric left-right signaling in vertebrate heart and gut looping. *Development* **126**, 1225-1234.
- Collignon, J., Varlet, I. and Robertson, E. J. (1996). Relationship between asymmetric *nodal* expression and the direction of embryonic turning. *Nature* **381**, 155-158.
- Danos, M. C. and Yost, H. J. (1995). Linkage of cardiac left-right asymmetry and dorsal-anterior development in *Xenopus*. *Development* **121**, 1467-1474.
- Danos, M. C. and Yost, H. J. (1996). Role of notochord in specification of cardiac left-right orientation in zebrafish and *Xenopus*. *Dev. Biol.* **177**, 96-103.
- Dufort, D., Schwartz, L., Harpal, K. and Rossant, J. (1998). The transcription factor HNF3beta is required in visceral endoderm for normal primitive streak morphogenesis. *Development* **125**, 3015-3025.
- Echelard, Y., Epstein, D.J., St-Jacques, B., Shen, L., Mohler, J., McMahon, J.A. and McMahon A.P. (1993). Sonic hedgehog, a member of a family of putative signaling molecules, is implicated in the regulation of CNS polarity. *Cell* **75**, 1417-1430.
- Gebbia, M., Ferrero, G. B., Pilia, G., Bassi, M. T., Aylsworth, A. S., Penman-Splitt, M., Bird, L. M., Bamforth, J. S., Burn, J., Schlessinger, D., Nelson, D. L. and Casey, B. (1997). X-linked situs abnormalities result from mutations in *ZIC3*. *Nature Gen.* **17**, 305-308.
- Gee, M. A., Heuser, J. E. and Vallee, R. B. (1997). An extended microtubule-binding structure within the dynein motor domain. *Nature* **390**, 636-639.
- Gibbons, I. R., Gibbons, B. H., Mocz, G. and Asai, D. J. (1991). Multiple nucleotide-binding sites in the sequence of dynein b heavy chain. *Nature* **352**, 640-643.
- Goldstein, A. M., Ticho, B. S. and Fishman, M. C. (1998). Patterning the heart's left-right axis: from zebrafish to man. *Dev. Genet.* **22**, 278-287.
- Handel, M. A. and Kennedy, J. R. (1984). *Situs inversus* in homozygous mice without immotile cilia. *J. Hered.* **75**, 498.

- Heymer, J., Kuehn, M. and Ruther, U. (1997). The expression pattern of nodal and lefty in the mouse mutant Ft suggests a function in the establishment of handedness. *Mech. Dev.* **66**, 5-11.
- Holzbaur, E. L. F. and Vallee, R. B. (1994). Dyneins: molecular structure and cellular function. *Annu. Rev. Cell Biol.* **10**, 339-372.
- Hummel, K. P. and Chapman, D. B. (1959). Visceral inversion and associated anomalies in the mouse. *J. Hered.* **50**, 9-13.
- Hyatt, B. A. and Yost, H. J. (1998). The left-right coordinator: the role of Vg1 in organizing left-right axis formation. *Cell* **93**, 37-46.
- Isaac, A., Sargent, M. G. and Cooke, J. (1997). Control of vertebrate left-right asymmetry by a Snail-related zinc finger gene. *Science* **275**, 1301-1304.
- Israeli, S., Lowe, L.A., Bertness, V., Good, D.J., Dorward, D.W. Kirsch, I.R. and Kuehn, M.R. (1999) The SIL gene is required for mouse embryonic axial development and left-right specification. *Nature* **399**, 691-694.
- Kandl, K. A., Forney, J. D. and Asai, D. J. (1995). The dynein genes of *Paramecium tetraurelia*: the structure and expression of ciliary β and cytoplasmic heavy chains. *Mol. Biol. Cell* **6**, 1549-1562.
- King, T., Beddington, R. S. P. and Brown, N. A. (1998). The role of the brachyury gene in heart development and left-right specification in the mouse. *Mech. Dev.* **79**, 29-37.
- Klar, A. J. S. (1994). A model for specification of the left-right axis in vertebrates. *Trends Genet.* **10**, 392-396.
- Layton, W. M. (1976). Random determination of a developmental process. *J. Hered.* **67**, 336-338.
- Levin, M., Johnson, R. L., Stern, C. D., Kuehn, M. and Tabin, C. (1995). A molecular pathway determining left-right asymmetry in chick embryogenesis. *Cell* **82**, 803-814.
- Levin, M., Pagan, S., Roberts, D. J., Cooke, J., Kuehn, M. R. and Tabin, C. J. (1997). Left/right patterning signals and the independent regulation of different aspects of situs in the chick embryo. *Dev. Biol.* **189**, 57-67.
- Levin, M. and Mercola, M. (1998). The compulsion of chirality: toward an understanding of left-right asymmetry. *Genes Dev.* **12**, 763-769.
- Logan, M., Pagan-Westphal, S. M., Smith, D. M., Paganessi, L. and Tabin, C. J. (1998). The transcription factor Pitx2 mediates situs-specific morphogenesis in response to left-right asymmetric signals. *Cell* **94**, 307-317.
- Lohr, J. L., Danos, M. C. and Yost, H. J. (1997). Left-right asymmetry of a nodal-related gene is regulated by dorsoanterior midline structures during *Xenopus* development. *Development* **124**, 1465-1472.
- Lowe, L. A., Supp, D. M., Sampath, K., Yokoyama, T., Wright, C. V. E., Potter, S. S., Overbeek, P. and Kuehn, M. R. (1996). Conserved left-right asymmetry of nodal expression and alterations in murine situs inversus. *Nature* **381**, 158-161.
- Marszalek J.R., Ruiz-Lozano P., Roberts E., Chien K.R. and Goldstein L.S. (1999) Situs inversus and embryonic ciliary morphogenesis defects in mouse mutants lacking the KIF3A subunit of kinesin-II. *Proc. Natl. Acad. Sci. USA* **96**, 5043-5048.
- McNeish, J. D., Thayer, J., Walling, K., Sulik, K. K., Potter, S. S. and Scott, W. J. (1990). Phenotypic characterization of the transgenic mouse insertional mutation, legless. *J. Exp. Zool.* **253**, 151-162.
- Melloy, P. G., Ewart, J. L., Cohen, M. F., Desmond, M. E., Kuehn, M.R. and Lo, C. W. (1998). No turning, a mouse mutation causing left-right and axial patterning defects. *Dev. Biol.* **193**, 77-89.
- Meno, C., Saijoh, Y., Fujii, H., Ikeda, M., Yokoyama, T., Yokoyama, M., Toyoda, Y. and Hamada, H. (1996). Left-right asymmetric expression of the TGF β -family member lefty in mouse embryos. *Nature* **381**, 151-155.
- Meno, C., Shimono, A., Saijoh, Y., Yashiro, K., Mochida, K., Ohishi, S., Noji, S., Kondoh, H. and Hamada, H. (1998). Lefty-1 is required for left-right determination as a regulator of lefty-2 and nodal. *Cell* **94**, 287-297.
- Metzler, M., Gertz, A., Sarkar, M., Schachter, H., Schrader, J. W. and Marth, J. D. (1994). Complex asparagine-linked oligosaccharides are required for morphogenic events during post-implantation development. *EMBO J.* **13**, 2056-2065.
- Morris R. L. and Scholey J. M. (1999). Heterotrimeric kinesin-II is required for the assembly of motile 9+2 ciliary axonemes on sea urchin embryos. *J. Cell Biol.* **138**, 1009-1022.
- Nonaka, S., Tanaka, Y., Okada, Y., Takeda, S., Harada, A., Kanai, Y., Kido, M. and Hirokawa, N. (1998). Randomization of left-right asymmetry due to loss of nodal cilia generating leftward flow of extraembryonic fluid in mice lacking KIF3B motor protein. *Cell* **95**, 829-837.
- Pagan-Westphal, S. M. and Tabin, C. J. (1998). The transfer of left-right positional information during chick embryogenesis. *Cell* **93**, 25-35.
- Piedra, M. E., Icardo, J. M., Albajar, M., Rodriguez-Rey, J. C. and Ros, M. A. (1998). Pitx2 participates in the late phase of the pathway controlling left-right asymmetry. *Cell* **94**, 319-324.
- Ryan, A. K., Blumberg, B., Rodriguez-Esteban, C., Yonei-Tamura, S., Tamura, K., Tsukui, T., de la Pena, J., Sabbagh, W., Greenwald, J., Choe, S., Norris, D. P., Roberston, E. J., Evans, E. M., Rosenfeld, M. G. and Belmonte, J. C. I. (1998). Pitx2 determines left-right asymmetry of internal organs in vertebrates. *Nature* **394**, 545-551.
- Sefton, M., Sanchez, S. and Nieto, M. A. (1998). Conserved and divergent roles for members of the Snail family of transcription factors in the chick and mouse embryo. *Development* **125**, 3111-3121.
- Splitf, M. P., Burn, J. and Goodship, J. (1996). Defects in the determination of left-right asymmetry. *J. Med. Genet.* **33**, 498-503.
- Srivastava, D. (1997). Left, right... which way to turn? *Nat. Genet.* **17**, 305-308.
- Supp, D. M., Witte, D. P., Branford, W. W., Smith, E. P. and Potter, S. S. (1996). Sp4, a member of the Sp1-family of zinc finger transcription factors, is required for normal murine growth, viability, and male fertility. *Dev. Biol.* **176**, 284-299.
- Supp, D. M., Witte, D. P., Potter, S. S. and Brueckner, M. (1997). Mutation of an axonemal dynein affects left-right asymmetry in inversus viscerum mice. *Nature* **389**, 963-966.
- Takeda, S., Yonekawa, Y., Tanaka, Y., Okada, Y., Nonaka, S. and Hirokawa, N. (1999). Left-right asymmetry and kinesin superfamily protein KIF3A: new insights in determination of laterality and mesoderm induction by *kif3A*^{-/-} mice analysis. *J. Cell Biol.* **145**, 825-836.
- Vogan, K. J. and Tabin, C. J. (1999). A new spin on handed asymmetry. *Nature* **397**, 295-298.
- Wheatley, D. N., Wang, A. M. and Strugnell, G. E. (1996). Expression of primary cilia in mammalian cells. *Cell Biol. Inter.* **20**, 73-81.
- Yokoyama, T., Copeland, N. G., Jenkins, N. A., Montgomery, C. A., Elder, F. F. B. and Overbeek, P. A. (1993). Reversal of left-right asymmetry; a situs inversus mutation. *Science* **260**, 679-682.
- Yoshioka, H., Meno, C., Koshiba, K., Sugihara, M., Itoh, H., Ishimaru, Y., Inoue, T., Ohuchi, H., Semina, E. V., Murray, J. C., Hamada, H. and Noji, S. (1998). Pitx2, a bicoid-type homeobox gene, is involved in a lefty-signaling pathway in determination of left-right asymmetry. *Cell* **94**, 299-330.